Introducing the near infrared VLTI instrument AMBER to its users

Romain Petrov

INTRODUCING THE NEAR INFRARED VLTI INSTRUMENT AMBER TO ITS USERS

ROMAIN G. PETROV
Universite de Nice-Sophia Antipolis, Parc Valrose, F-06108 Nice, France
E-mail: petrov@unice.fr

THE AMBER CONSORTIUM[†]
Universite de Nice-Sophia Antipolis, Parc Valrose, F-06108 Nice, France
Observatoire de la Cote d'Azur, BP 4229, F-06304 Nice, France
Universite Joseph Fourier, BP53, F-38041 Grenoble, France
Max Planck Institute fur Radiosatronomie, Auf den Huegel 69, D-53121 Bonn, Deutschland
Osservatorio Astrofisico di Arcetri, Largo E. Fermi 5, I-50125 Firenze, Italia

Abstract. AMBER is the General User near infrared focal instrument of the Very Large Telescope Interferometer. It is a single mode, dispersed fringes, three telescope instrument. A limiting magnitude of the order of H=13 will allow tackling of a fair sample of extra galactic targets. A very high accuracy, in particular in color differential phase and closure phase modes gives good hope for very high dynamical range observations, possibly including hot extra solar planets. The relatively high maximum spectral resolution, up to 10000, will allow stellar activity observations. Between these extreme goals, AMBER has a wide range of applications including Young Stellar Objects, Evolved Stars, circumstellar material and many others.

Keywords: astronomy, optical interferometry, instrumentation, high angular resolution, very large telescope, differential interferometry

1. Introduction

AMBER is a near infrared, three beam, dispersed fringes, single mode, focal instrument for the interferometric mode of the Very Large Telescope (VLTI). The VLTI (Glindemann et al., 2002) feeds AMBER with two or three beams produced by any of the telescopes present on the Paranal Mountain top. Each beam has been partially corrected for atmospheric turbulence and is stabilized in direction, position and optical path. Besides a very wide scientific program (Malbet et al., 2002a), the near infrared offers the possi bility to use nearly diffraction limited images. The three beams yield closure phases, which have interesting calibration properties and offer the possibility to reconstruct images. Still, AMBER will mainly be an efficient 'model fitting' instrument thanks to its large spectral coverage, from 1.1 to 2.4 μm and spectral resolutions (35, 1000 and 10000). The dispersed fringes increase: the

[†] The AMBER Consortium has been established by the five Institutes in the affiliation list and is supported by more than 50 engineers and researchers. More information can be found on the web site: `www.obs-nice.fr/amber`

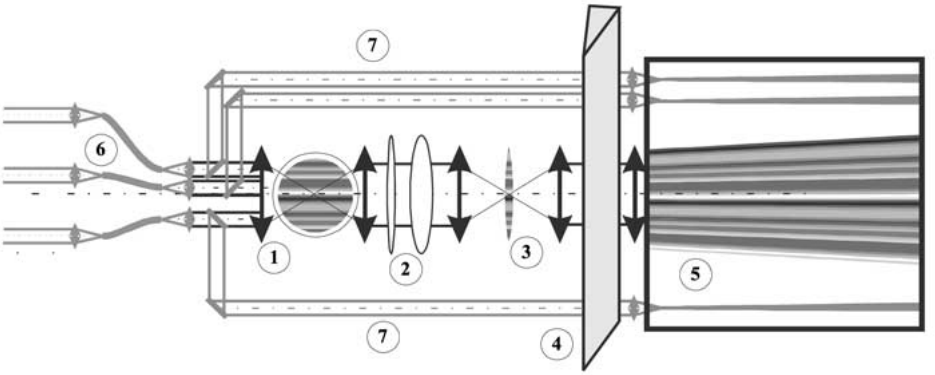

Figure 1. Basic concept of AMBER. 1: multi axial beam combiner; 2: cylindrical optics; 3: anamorphotic image in spectrograph slit; 4: spectrograph; 5: dispersed fringes on 2D Hawaii detector; 6: spatial filtering of incoming beams with single mode fibers; 7: channels for photometric monitoring.

instantaneous frequency plane coverage; the instrument accuracy when a (set of) spectral channel(s) can be used as a reference. They allow measures on unresolved and/or very high dynamics systems. The spatial filtering with single mode fibers is intended to achieve the highest possible accuracy on absolute as well as on differential visibility measurements.

Figure 1 summarizes the key elements of the AMBER concept. AMBER has a multi axial beam combiner (1) which produces fringes in the Airy pattern common to several non-redundantly spaced parallel beams. A cylindrical optics system (2) feeds this Airy pattern into the entrance slit (3) of a spectrograph (4), which disperses the fringes on an array detector (5). The medium (1000) and highest (10000) spectral resolutions imply to cool the spectrograph and to equip it with cold slits and pupil stops. Each incoming beam goes through a single mode optical fiber (6) which reduces all atmospheric and optic aberrations into an unknown optical path difference (OPD), which can be frozen, and an unknown coupling factor into the fibers. The coupling factors are monitored in real time by photometric beams (7) which analyze at each wavelength the transmitted flux. Since a single mode fiber is efficient only over a limited wavelength range, before feeding the beams in the fibers we split the total spectral range with dichroics and we have different spatial filters for the J, H and K bands. In addition to these basic features AMBER is equipped with many beam cleaning tools (polarization filters, refraction and dispersion correctors...) and calibration devices (artificial coherent sources, calibrated phase delays, beam commuters...). More details about the instrument can be found in (Petrov et al., 2002a; Malbet et al., 2002b; Chelli et al., 2002).

2. Amber Measurements and Science

By reconfiguring the VLTI ATs over the available Paranal summit positions, good use of super synthesis and of the increase in u-v sampling due to our large wavelength coverage permits reconstructing an image at the diffraction limit of the interferometer. However, such a process will be quite slow and future AMBER users should mainly think about it as an instrument designed to constrain models of astrophysical sources thanks to a limited number of angular measurements with a rich wavelength information. The following paragraphs explain what are the key AMBER measurements, together with some examples of the kind of information they can provide and with their main calibration requirements and methods.

2.1. AMBER MEASUREMENTS

For each elementary frame and in each AMBER spectral channel, we have an interferometric and three photometric signals processed by the same optics and the same dispersive elements. After the correction of detector cosmetics and background subtraction, a generalization of the ABCD algorithm is used (Chelli et al., 2002) to establish a linear relation between the values measured in each pixel and the complex coherence for each baseline. The matrix is calibrated using artificial sources and records of various interferograms affected by different known phase delays. It combines the effects of many parameters such as the detector gain table and bad pixels, the exact shape of the beams after the fiber output and the pupil stop in the spectrograph. For each baseline l-m, we measure the visibility $V_{lm}(\lambda)$ and the phase $\Phi_{lm}(\lambda)$.

2.1.1. *Calibrated visibility as a function of wavelength:* $V_{lm}(\lambda)$

After time averaging and various bias corrections and calibration steps (Chelli et al., 2002), $V_{lm}(\lambda)$ yields the calibrated visibility in each spectral channel. For a simple object, $V_{lm}(\lambda)$ will give constraints on its angular size in the direction of the baseline B_{lm}. If a certain range of spatial frequencies B_{lm}/λ is explored, thanks to baseline changes or to the spectral coverage, visibility measurements yield the different scales of the structures present in the source. Several levels of attenuation at different spatial frequencies can indicate that structures of various sizes are present. For example the super giant star Betelgeuse shows at first very fast visibility attenuation with frequency, which is the signature of an extended dust envelope. At higher frequencies, a limb darkened disk model can fit a fraction of the visibility curve. Finally, at the highest frequencies, where the disk contribution is expected to be very low, the visibility remains significantly higher than zero, which can be interpreted as the signature of a structure smaller than the stellar disk such as a stellar spot.

The use of measurements at different wavelengths increases the frequency coverage and can constrain the interpretation. For example, in a circumstellar envelope

or an AGN BLR, one can compare the visibility in two narrow spectral channels in a spectral line. Each spectral channel corresponds to an area of given radial velocity. The comparison between the measures constrains the relative sizes of the equal velocity areas and the velocity field (Marconi et al., 2002).

The accuracy of the visibility measurements is critical. A few % accuracy yields gross size information (which in a limited number of cases can be very valuable). But, for example, limb darkening or different radial distribution of material in an envelope or in a dust torus will produce visibility variations of the order of 1% or less. Detecting features which are faint or small with regard to a main source (binary stars with a strong magnitude difference and ultimately extra solar planets, star spots, structures in envelopes or disks...) is particularly demanding. Even the hottest giant extra solar planets such as 51 Peg, have visibility signatures smaller than 10^{-4}. The same will apply for 'planetary gaps' in accretion disks or for stellar structures on otherwise quite unresolved stars. In spite of all precautions: single mode spatial filtering, frozen piston, short exposures and dispersion correction, the visibility will still be sensitive to instrumental and atmospheric effects. The main tool to calibrate it is to observe as often as possible a reference star with unit or known visibility. The fundamental limit comes from the speed with which is it possible to switch between science and reference source, and to lock AOs and fringe tracker on both sources. Our best expectation for the period of such a calibration cycle is 10 minutes (closer to 30 minutes in the first months or years of VLTI operation).

2.1.2. *Differential visibility and phase*

One or several spectral channels can be defined as being a reference channel (when several wavelengths are used, the information is averaged over λ). Then the ratio between the visibility in each spectral channel and the visibility in the reference channel yields the differential visibility $V_{lm}(\lambda)/V_{lm}(\lambda_0)$. The interesting point is that $V_{lm}(\lambda)$ and $V_{lm}(\lambda_0)$ are measured simultaneously which increases the accuracy of the calibration since many effects will affect all the channels in the same way (or in ways related by known equations). The absolute phase $\Phi(\lambda)$ has no meaning unless an absolute metrology (Glindemann et al., 2002) is available. However, it is immediately possible to measure the absolute phase differences between any spectral channel and the reference channel: $\Phi_{lm}(\lambda) - \Phi_{lm}(\lambda_0)$. The Differential Phase can bring specific astrophysical information. For example, if one observes in different channels of a line as described above, the Differential Phase will constrain the angular distance between the two different velocity areas. For sources with relatively simple or partially known velocity fields combining the variation of the visibility modulus and phase with wavelength is particularly interesting. The modulus variation will constrain the relative sizes and intensities of the equal velocity zones while the phase will constrain their relative position. Combining these values with some knowledge of the velocity field can allow to almost reconstruct images. A good example is likely to be circumstellar envelopes or AGN observed

in emission lines (Marconi et al., 2002). Among many other applications we have multiple system with small number of stars, envelopes combining a global rotation and a global expansion, knots in a jet with a similar global direction but different velocities... Both Differential measurements are particularly interesting when the object is known to be unresolved in some spectral channels and resolved in others. Then, if the channel containing an unresolved source is used for reference, the differential complex visibility in the other channels is the exact object visibility and the image reconstruction process can be as efficient as if we had a 'phase referencing system'. A specific interest of the differential phase is that, unlike the differential modulus, it can be calibrated using an internal modulation instead of an external reference star. The measured phase difference $\Delta\Phi_{lm}(\lambda)$ will be the sum of:

$$\Delta\Phi_{lm}(\lambda) = \Delta\Phi_{lm,*}(\lambda) + \Delta\Phi_{lm,a}(\lambda) + \Delta\Phi_{lm,I}(\lambda) \quad (1)$$

where $\Delta\Phi_{lm,*}(\lambda)$ is due to the source, $\Delta\Phi_{lm,a}(\lambda)$ is the contribution of the atmosphere, which is very strongly dominated by the differential dispersion in the tunnels and $\Delta\Phi_{lm,I}(\lambda)$ is the instrumental chromatic phase difference between the beams l and m. The dominant and most difficult to eliminate term is the instrumental one $\Delta\Phi_{lm,I}(\lambda)$. AMBER plans to solve this problem by inverting the beams as close as possible to the entrance of the instrument, before any chromatic optics in AMBER (dichroics, fibers, beam splitters, cryostat windows, spectrograph chamber, detector...). Then we obtain a new phase difference $\Delta\Phi_{ml}(\lambda)$:

$$\Delta\Phi_{ml}(\lambda) = -\Delta\Phi_{lm,*}(\lambda) - \Delta\Phi_{lm,a}(\lambda) + \Delta\Phi_{lm,I}(\lambda) \quad (2)$$

The difference between equations (1) and (2) eliminates the instrumental term $\Delta\Phi_{lm,I}(\lambda)$. The atmospheric term $\Delta\Phi_{lm,a}(\lambda)$ results from the differences in average temperature, pressure and water vapor be tween the two beams. The first two terms have a globally multiplicative effect, except for saturated water vapor lines, and can be fitted in the data itself particularly if we use a large spectral coverage.

It has been shown (Vannier et al., 2002) that if we have differential phase measurements with the UTs, at low spectral resolution over the full J,H,K spectral coverage, limited only by photon, background and detector noise, the variation of phase with wavelength produced by the presence of a Jupiter mass hot extra solar planet around a solar type star at 10 pc can be detected. The SNR will be higher than 20 for 51 Peg (separation = 0.05 AU) and the SNR will be around two for a separation of about 0.2 AU. Such an observation will yield: the orbital parameters and thus the mass of the planet; the spectrum and thus the temperature and composition of the planet atmosphere. These measurements are one of the most ambitious AMBER goals, since the corresponding phase variation ranges between a few 10^{-5} and a few 10^{-4} radians. The conditions to achieve such an extreme accuracy are that the instrumental and atmospheric variation must be smaller than the photon noise over the calibration period. After a systematic study of all factors affecting this measurement (Vannier et al., 2002) it appears that the result is achievable with

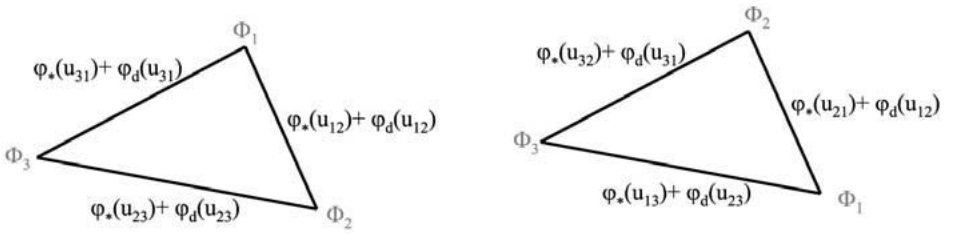

Figure 2. Closure phase before and after beam commutation.

a 30 s calibration cycle based on an internal beam commutation and out of reach if one has to use the 300 s cycle using a reference star. A specific attention has to be dedicated to the atmosphere term, which is not corrected by the beam commutation. As explained above, with two telescopes we expect to compute this term from the data itself. If this fails, with three telescopes this dispersion term can be eliminated using the closure phase relation (Segransan et al., 2001).

2.1.3. *Closure phase* $\Phi_{123}(\lambda)$
In the closure phase relation:

$$\Phi_{123}(\lambda) = \Phi_{12}(\lambda) + \Phi_{23}(\lambda) + \Phi_{31}(\lambda)$$

all atmospheric and most of instrumental terms are cancelled. The exceptions result from the fringe detection process (error in the 'pixel to visibility' matrix (PTVM) due to a change in the detector gain table, in the beams shape or overlap after the fibers, in the spectrograph geometry...). Fortunately, we recently discovered (Petrov et al., 2002b) that commuting two of the three beams calibrates the closure phase relation. Let's assume that we measure the phases for the three baselines B12, B23 and B31. Each beam i is affected by an optical path difference (OPD) which translates in a phase Φ_i. The spatial frequency $u_{lm} = B_{lm}/\lambda$ yields the sum of source phase $\phi_*(u_{lm})$ with a detection phase error $\phi_d(u_{lm})$, as illustrated in Figure 2.

Since $\phi_*(u_{ij}) = -\phi_*(u_{ji})$ and $\phi_d(u_{ij}) = -\phi_d(u_{ji})$, the difference between the closure phase $\Phi_{123}(\lambda)$ without and $\Phi'_{123}(\lambda)$ with commuting beams 1 and 2 yields

$$\left(\Phi_{123}(\lambda) - \Phi'_{123}(\lambda)\right)/2 = \phi_*(u_{12}) + \phi_*(u_{23}) + \phi_*(u_{31}) = \phi_{*,123}(\lambda) \qquad (3)$$

where $\phi_{*,123}(\lambda)$ is an astronomical closure phase measurement free from any atmospheric or instrumental effect, if the beam commutation has been made fast enough for the instrumental terms to remain unchanged. This way to obtain a perfectly calibrated closure phase is unique to the VLTI because of its three large telescopes and to AMBER because of its beam commuting device. In addition to this very interesting calibration 'perfection', the closure phase is the key for image

reconstruction. Moreover, even a limited number of closure phases can strongly constrain a model. For example a zero closure phase at medium frequencies and a non zero one at higher frequencies may indicate (and allow to locate) a small non symmetric feature on an otherwise globally symmetric object.

2.1.4. *Differential photocenter*

When the source is unresolved (i.e. smaller than B/λ) the phase tends to be proportional to the photocenter of the object at that given wavelength: $\Phi_{lm}(\lambda) = 2\pi(\vec{B}_{lm}/\lambda).\vec{\epsilon}(\lambda)$, where $\vec{B}_{lm}.\vec{\epsilon}(\lambda)$ is the scalar product of the two vectors. The photocenter is defined as the barycenter of the object brightness distribution $o(r, l)$ at the wavelength λ:

$$\epsilon(\lambda) = \frac{\int r\, o(r,l)\, dr}{\int o(r,l)\, dr} \tag{4}$$

Since phase differences can be measured even when they are extremely small compared to 2π, this allows to extract, from differential phases, the variation of objects photocenter as a function of wavelength; even when the source is much smaller than the resolution limit. For example, for a magnitude 5 source observed with a resolution 1000 during 5 hours with an UT, one can measure photocenter displacement of about 0.1 μas. For a magnitude 10 star with UTs or a magnitude 7 star with ATs the accuracy on the photocenter displacement remains 1 μas for the same resolution 1000. This allows obtaining information on sources or structures much smaller than the resolution limit, such as stellar spots (Petrov, 1989).

One of the most interesting applications is likely to be the study of the Broad Line Regions (BLR) of Active Galactic Nuclei (Marconi et al., 2002). The study of the photocenter has numerous other applications, including stellar rotation, differential rotation, position of stellar rotation axes in multiple systems, stellar diameters of otherwise unresolved objects, asteroseismology, cepheids, structure and kinematics of unresolved disks and envelopes... The key fact to remember is that for objects with spatially structured spectral features, the limiting resolution of the AMBER/VLTI can be much smaller than the classical B/λ (1 or 2 mas) limit. Photocenter measurements of unresolved objects are linked to differential phase measurements because it is easy to show that when a source of angular size a is unresolved, the photocenter and the differential phase decrease proportionally to a, while the visibility modulus approaches 1 like a^2 and the closure phase decreases like a^3.

2.2. Observing and calibration cycles of AMBER

The observing modes of AMBER are set by: the number of telescopes (2 or 3); the spectrograph set up (resolutions ≈ 35; ≈ 1000 ; ≈ 10000 ; spectral coverage; central wavelength); the availability of a fringe tracker. It seems that, from the very beginning, AMBER observations will benefit from an on axis fringe tracker (FINITO (Gai, 2001)).

In all cases the observing and data processing sequences remain the same and are defined by the following parameters.

- The required accuracy: for very precise measurements of the visibility modulus, one should use very short frame times, even with a fringe tracker. The minimum frame time is of the order of 10 ms for 40 spectral channels (J,H and K band in the low resolution mode). For higher sensitivity (and lower accuracy except in the differential modes) one could use longer frame times (50 to 100 ms) even with poor fringe tracking. Finally for high spectral resolution, correct fringe tracking must support frame times up to a few tens of seconds.
- The kind of calibration selected: visibility measurements will give priority to frequent calibration using one or more reference stars. Differential measurement will use relatively fast internal beam commutation and use external reference stars only from time to time to check the instrument.

In all these very similar modes, we set up the instrument and perform the corresponding PTVM calibration. Then we read frames, with frame times selected as explained above, and we combine them in exposures (successive frames recorded on the same source with the same instrument set up). Each exposure yields measurements of the complex coherence but a complete calibration needs a combination of exposures of different sources (science target, reference star, sky background, calibration lamps...) or with different beam commutations. All sequences of operations needed to perform a given measurement, i.e. a given exposure cycle, are automatically executed by the instrument. The sequences are described in standard templates, with parameters set by the User as a function of its scientific objectives. For each given exposure cycle there is a standard way to reduce the data for calibrated measurements, which will be delivered to the standard User. However, all data will be recorded to allow more sophisticated post processing.

2.3. SUMMARY OF AMBER TOP LEVEL SPECIFICATIONS AND EXPECTED PERFORMANCES

Table I summarizes the main specifications of AMBER after the various tradeoffs made during the design phases.

The fringe tracker sets the limiting magnitude of AMBER. The current conservative estimate for $\lambda/20$ fringe tracking is H = 13. Table II gives the SNR which can be expected in each spectral channel on a source with visibility close to 1. We assumed 4 hours observations divided in 50 to 100 s frames for a star of magnitude H=12 with the UTs or H=9 with the ATs, for various spectral resolutions. It is important to remember that: the error in the differential phase can be estimated to be $\sigma_\phi = 1/(\sqrt{2}\mathrm{SNR})$ radians; the error in the photocenter displacement is given by $\sigma_\epsilon = \sigma_\phi(\lambda/B)/2\pi$; for lower visibility sources, the SNR decreases with the visibility modulus.

For example, for a magnitude H=12, at resolution 1000 we will get $\sigma_\phi = 3 \times 10^{-3}$ radians and $\sigma_\epsilon = 2\,\mu$arcsec (K band, 100 m baseline), which is suf-

TABLE I

Summary of the top level specifications of AMBER

Characteristic	Specification	Goal
Number of beams	3	
Spectral resolution R	$\approx$ 35, 1000 and 10000 in K band, 2nd order in J, intermediate in H	
Spectral coverage	J,H,K from 1 to 2.4 μm	
Instantaneous spectral coverage	Simultaneous observation of the full spectral domain for $R = 35$	
Instrument contrast	0.8	0.9
Absolute visibility accuracy	$3\sigma_V = 0.01$	$\sigma_V = 10^{-4}$
Differential visibility accuracy	$3\sigma_{V/V_0} = 10^{-3}$	$3\sigma_{V/V_0} = 10^{-4}$
Differential phase accuracy	$3\sigma_{\Delta\Phi} = 10^{-3}$ rad	$\sigma_{\Delta\Phi} = 10^{-5}$ rad
Instrument contrast stability	10^{-2} over 5 minutes	10^{-3} over 5 minutes
Differential phase stability	10^{-3} rad over 1 minute	10^{-4} rad over 1 minute

TABLE II

SNR (or $1/\sigma_V$ or $1/\sqrt{2}\sigma_\phi$) per spectral channel for a star of magnitude H=12 (left, fringe tracking limit) with the UTs or H=7 (right) with the UTs (and 3 magnitudes less with the ATs). 4 hours of observation divided in 50 s frames

Telescopes and star magnitude	UTs (H=12) or ATs (H=9)			UTs (H=7) or ATs (H=4)		
Bands	J	H	K	J	H	K
Resolution = 35	508	843	1111	5080	8430	11110
Resolution = 1000	95	158	208	950	1580	2080
Resolution = 10000	30	50	66	300	500	660

ficient to resolve all quasars and Seyfert 1 BLRs with these kind of magnitudes. Another example, is that for a magnitude 7 star, we should have at resolution 35, a differential phase error $\sigma_\phi = 6 \times 10^{-5}$ radians, sufficient to resolve many 51 Peg like planets, if of course we manage to be limited only by these fundamental noises.

Eventually, a field separator will allow tracking of fringes and measuring wavefronts on stars up to 1 minute away from the science source. When such a reference source exists, the limiting magnitude of AMBER can approach 20 in a few hours. However, with the current performance of fringe trackers, the corresponding sky coverage will be very poor. To have good sky coverage, we need fringe sensors with

detectors limited by photon noise in the near infrared. This might be achievable in a few years.

3. Conclusion

All subsystems of AMBER have been delivered and are now in the final global integration and test phase. The first fringes in the K band with all instrument components have been obtained in January 2003. We expect to ship the instrument to Paranal during the summer 2003, after a full laboratory commissioning of the hardware and the software. The commissioning with two large telescopes (UTs with Adaptive Optics) should take place before the end of the year and a partial access to the instrument offered to the Consortium and to the Community starting in April 2004. The full operation with three telescopes will probably be open in October 2004. The summary of the AMBER consortium Guaranteed Time Program will be released in April 2003. The initial pressure factor was of about two on the UTs and three on the ATs and we had to make a severe selection. We now have two proposals about the distance scale in the Universe, 15 extra galactic programs, mainly about Quasars and other AGNs, 22 programs about Star formation covering many topics such as parameters of PMS stars, disks, outflows, jets, young binaries and young stellar clusters. Ten programs are about low-mass companions, with a very developed program on Pegasides planets. More than 22 programs tackle various aspects of the late stages of stellar evolutions and about 15 programs are dedicated on fundamental properties of stars (age, diameters, rotation, activity, seismology, magnetism) and of stellar envelopes (structure and kinematics). The UTs are mainly asked for extra galactic sources and extra solar planets. This leaves a lot of objects and room for additional programs and ideas and we are quite confident that AMBER will permit a large harvest of new results.

References

Chelli, A., Tatulli, E., Malbet, F. et al.: 2002, AMBER data processing, *SPIE* conference **4838** Interferometry for Optical Astronomy II, Waikoloa, Hawaii, USA, 2002, in publication.

Gai, M., Bonino, D., Corcione, L. et al.: 2001, in: J. Bergeron and G. Monnet (eds.), *FINITO: A Fringe Sensor for the VLTI in Two and Three Beam Configuration*, ESO symposia Scientific drivers for ESO future VLT/VLTI instrumentation, pp. 328–330.

Glindemann, A., Ballester, P., Bauvir B. et al.: 2002, Very large telescope interferometer: a status report, *SPIE conference* **4838** Interferometry for Optical Astronomy II, Waikoloa, Hawaii, USA, 2002, in publication.

Malbet, F., Bloecker, T., Foy, R. et al.: 2002, Astrophysical potential of the AMBER/VLTI instrument, *SPIE* conference **4838** Interferometry for Optical Astronomy II, Waikoloa, Hawaii, USA, 2002, in publication.

Malbet, F., Petrov, R.G., Tallon-Bosc, I. et al.: 2002, System analysis of the AMBER instrument on VLTI, *SPIE* conference **4838** Interferometry for Optical Astronomy II, Waikoloa, Hawaii, USA, 2002, in publication.

Marconi, A., Maiolino, R. and Petrov, R.G.: 2002, Extragalactic astronomy with the VLTI: a new window on the universe, *Proceedings of JENAM 2002 Conference*, Porto, Portugal, September 2002 (these proceedings).

Petrov, R.G.: 1989, Differential interferometry, in: D. Alloin and J.M. Mariotti (eds.), *Diffraction Limited Imaging with Very Large Telescopes*, NATO ASI Series C, **274**, Kluwer. Ac., pp. 249, 272.

Petrov, R.G., Malbet, F., Weigelt, G. et al.: 2002, Using the near infrared VLTI instrument AMBER, *SPIE* conference **4838** Interferometry for Optical Astronomy II, Waikoloa, Hawaii, USA, 2002, in publication.

Petrov, R.G., Vannier, M., Lopez, B., Bresson, Y., Robbe-Dubois, S. and Lagarde, S.: 2002, Orbits and spectra of extra solar planets with the VLTI focal instrument AMBER, in: G. Aime and R. Soumer (eds.), *Proceedings of the Workshop on Very High Dynamics Imagery and Extra Solar Planets*, Nice, France, May 2002. EDP Science Series.

Robbe-Dubois, S., Antonelli, P., Bresson, Y. et al.: 2002, VLTI focal instrument AMBER: results of the laboratory commissioning of the warm optics, *SPIE* conference **4838** Interferometry for Optical Astronomy II, Waikoloa, Hawaii, USA.

Segransan, D. et al.: 2001, How AMBER will contribute to the search of brown dwarfs and extrasolar planets, *SPIE* proceedings **4006**, Munich, March 2000, pp. 269–276.

Vannier, M., Petrov, R.G., Robbe-Dubois, S. et al.: 2002, Optimizing a Differential Interferometric Instrument, in: J. Bergeron and G. Monnet (eds.), *ESO Symposia Scientific Drivers for ESO Future VLT/VLTI Instrumentation*, pp. 340, 346.